Journal of Engineering Science and Technology
Vol. 9, No. 2 (2014) 176 - 190

ESTIMATION OF AERODYNAMIC PARAMETERS OF URBAN BUILDING ARRAYS USING WIND TUNNEL MEASUREMENTS

SHEIKH AHMAD ZAKI*,[1], AYA HAGISHIMA[2], JUN TANIMOTO[2], AHMAD FAIZ MOHAMMAD[1], AZLI ABD RAZAK[3]

[1] Malaysia-Japan International Institute of Technology, Universiti Teknologi Malaysia, 54100 Kuala Lumpur, Malaysia
[2] Interdisciplinary Graduate School of Engineering Sciences, Kyushu University, 6-1, Kasuga-koen,Kasuga-shi, Fukuoka 816-8580 Japan
[3]Faculty of Mechanical Engineering, Universiti Teknologi MARA, 40450 Shah Alam, Selangor, Malaysia
*Corresponding Author: sheikh@ic.utm.my

Abstract

The aim of this study is the experimental determination of a centre height of moment of drag force H_c, which is assumed to coincide with displacement height d on the basis of Jackson's theory. The authors performed a series of wind tunnel experiments on the spatial distribution of pressure drag acting on walls of rectangular block arrays arranged in staggered, square, and diamond layouts under the conditions of different roughness packing densities, i.e., 7.7%, 17.4%, 30.9%, and 39.1%. Total drag and wind profile of the arrays were preliminarily measured by a floating drag balance and a hot-wire anemometer, and roughness length z_o and d were derived using two-parameter fitting in our previous work. H_c values determined by the pressure drag measurement were compared with d of our previous work. The results show that the estimated H_c values for staggered and square arrays are significantly smaller than d except for the data of lowest packing density. Moreover, the z_o values estimated using one-parameter fitting and measured H_c are slightly larger than those of previous work for the three arrays with high packing density. Although inconsistencies of H_c and d exist, it is likely that H_c could be explained as d for a range of low packing densities, i.e., below 30.9%. The present results suggest the necessity of both more accurate data of spatially averaged wind profile and direct measurement of H_c for experimental determination of the roughness length and displacement height of a block array.

Keywords: Pressure drag, Wind tunnel, Roughness length, Displacement height.

Nomenclatures

C_d'	Bulk drag coefficient
C_p	Wind pressure coefficient
d	Displacement height, m
E	Mean wind speed, m/s
H	Height, m
H_c	Centre of height of the moment of drag force, m
i	Pressure tapping
L	Width, m
$\overline{M}$	Average of moment, Nm
n	Number of pressure tapping
P_b	Pressure on the back, N/m^2
P_f	Pressure on the front, N/m^2
U_i	Measured wind speed, m/s
U_δ	Free stream velocity, m/s
u*	Friction velocity, m/s
X	Distance of velocity, m
z_i	Height of pressure tapping, m
z_o	Roughness length, m

Greek Symbols

$\Delta\overline{P}$	*Average of pressure difference, N/m^2*
δ	Boundary layer depth, m
θ	Total momentum thickness
κ	von Karman's constant
λ_f	Frontal area density
λ_p	Plan area density
ρ	Density of air, kg/m^3
τ	Shear stress due to form drag, N/m^2

1. Introduction

The accurate estimation of aerodynamic parameters of urban rough surfaces, roughness length z_o and displacement height d, is important for prediction of air flow, dispersion of pollutants, and other atmospheric phenomena. However, the determination of these parameters still remains a difficult issue; Claus et al. [1] highlighted the difficulty of determining drag within rough surfaces whilst Kanda et al. [2] recently wrote that aerodynamic parameterizations though have been improved as research continues remains uncertain. In particular, the physical meaning of d is ambiguous and remains an open question. This is explained as we go through the different methods next.

Studies on aerodynamic parameters z_o and d for urban arrays with various geometry conditions have been carried out through various methodologies, including wind tunnel experiments and numerical simulations for several decades.

Basically, the accuracy of estimated z_o and d strongly depends on the determination of bulk drag force acting on a roughness array, (or drag coefficient or friction velocity u^*), which can be measured or estimated using several methods.

The first method is based on the measurement of the Reynolds stress within an inertial sub-layer known as covariance in the constant stress layer by cross-wire anemometry or laser Doppler velocimetry (e.g., Cook [3], Iyengar and Farell [4], Cheng and Castro [5], Salizzonni et al. [6]). The method presumes a constant-stress layer; however, the existence of constant-stress layer is not fully assured in a wall shear boundary layer developed in a wind tunnel or a computational domain. Actually, Cheng et al. [7] found that Reynolds shear stress in the inertial sub-layer is approximately 25% less than the surface shear stress deduced from pressure drag measurements.

In the second method, u^* is determined from the slope of the logarithmic velocity profile in the inertial sub-layer where $\frac{dU}{dz} = \frac{u*}{\kappa(z-d)}$ (e.g., Feddersen [8]). However, Feddersen [8] reported that the estimated errors of u^* in the inertial sub-layer are about 10% and 24% along the surface roughness length.

The third method is on the basis of the velocity defect law in the outer layer (e.g., Raupach et al. [9]) where flow is dependent on z_o, u^*, and boundary layer depth δ. The log-law profile in the outer layer can be defined as follows:

$$\frac{U_\delta}{u^*} = \frac{1}{\kappa}\ln\left(\frac{\delta}{z_o}\right) + B \tag{1}$$

where U_δ is the free stream velocity external to the boundary layer; B is the integration constant for the outer layer law, taken as 2.5.

This method relies on a canonical boundary layer in which the surface is uniform, the free stream is non-turbulent, the pressure gradient is zero, and the boundary layer is grown naturally without any tripping-up devices. Although theoretically it does not require an inertial sub-layer, the method is found to be effective only for heterogeneous array with sparse packing density within which interference effects are less than that of dense packing density. The fourth method estimates u^* from the integral momentum theory (e.g., Padhra [10]). The integral momentum method (von Karman [11]) is used to determine the amount of momentum lost between two streamwise locations, which are balanced against drag force under zero pressure gradient condition. The bulk drag coefficient, C_d' can be defined by using this method as follows (Padhra [10]):

$$C_d' = \frac{2\Delta\theta}{\Delta x} \tag{2}$$

where θ and x are the total momentum thickness and distance of velocity respectively for the shear stress profile within a boundary layer growing over a surface of two points.

Padhra [10] compared this method to Reynolds stress method, and found that both are not in good agreement for sparse and very dense arrays. In addition, the total errors in the momentum thickness and Reynolds stress method were found to be about 4% and 9%, respectively.

The fifth method is the direct measurement of drag force using floating drag balance installed in the wind tunnel. The different configurations of floating drag balance have been implemented in several studies; Maruyama [12] measured drag force imposed on a floating element above water using a strain gauge; Iyengar and Farell [4] used a floating element balance which consisted of two strain-gauge force sensors for direct measurements of wall shear stress; Mochizuki et al. [13] installed a floating element to which a mechanical device was attached for measurement; on the other hand, Cheng et al. [7] used gear oil for its high viscosity to effectively damp oscillation of the raft on which cubes were attached, and drag force was measured using a cantilever spring tethered to the raft; Hagishima et al. [14] and Zaki et al. [15] used a similar method with that of Maruyama [12] but with a floating element with plan area of 720 mm by 720 mm installed with a strain gauge to obtain total surface drag of each array. Friction velocity u^* was subsequently calculated; this study adopted the experimental value of u^* obtained in Hagishima et al. [14]. According to Iyengar and Farell [4], u^* determined from drag balance measurement is more accurate than using hot-wire anemometry mainly because it is more representative of a roughness array.

The last method is the direct measurement of form drag (e.g., Cheng et al. [7]), which we adopted. The measurement of form drag by Cheng et al. [7] was done by calculating the pressure difference of two opposing sides of a tapped cube. Integration of pressure differences over a frontal area of a cube yields form drag which is subsequently used to calculate friction velocity u^* as follows (Cheng et al. [7]):

$$u^* = \sqrt{\frac{\tau}{\rho}} \tag{3}$$

where τ and ρ are the surface shear stress due to form drag and air density respectively.

However, rather than obtaining u^*, this method was adopted by the authors especially to derive the centre height of moment drag force H_c using the pressure drag measurement as shown in Equation 5. By comparison, the other experimental measurements discussed earlier using cross-wire anemometry or laser Doppler velocimetry do not obtain drag force directly but Reynolds stress instead; hence, those methods are not appropriate to be applied in this study.

Meanwhile, methods to estimate z_o and d based on experimental data or numerical simulation can be classified into several approaches. The first approach uses the nonlinear least-squares method based on the logarithmic law from which the three parameters u^*, z_o, and d are simultaneously optimized by trial and error through curve fitting of the measured velocity profile. The parameter values are selected based on the results that best fit the statistical sense, the so-called "three-parameter fitting" (e.g., Antonia and Luxton [16], Theurer et al. [17]). Although this method has been successfully applied to determine u^* in a smooth wall boundary layer, their application to rough wall layer may yield rather inaccurate values of those three parameters.

In the second approach, z_o and d are estimated using non-linear least squares method based on the logarithmic law. This method is called "two-parameter fitting" (e.g., Cook [3], Iyengar and Farell [4], Cheng and Castro [5], Kanda et al. [18], Coceal et al. [19], Cheng et al. [7], Jiang et al. [20], Salizzonni et al. [6], Hagishima

et al. [14]), of which the value of u^* is separately obtained by one of the methods mentioned before. The fundamental approach of two-parameter fitting involves the determination of z_o and d by fitting the measured mean velocity profile near the ground surface to the logarithmic law (Cook et al. [3]). Then, the values of these two parameters are compared with those of other studies.

The third approach estimates z_o and u^* directly using log-law equation based on the data of mean streamwise velocity and Reynolds stress at a measurement point within the inertial sub-layer using the value of d predicted by Macdonald's simple method (e.g., Kanda and Moriizumi [21], Tomas et al. [22]).

In the fourth approach, d is derived from the measured pressure drag distribution using Jackson's theory [23] and z_0 is estimated using the log-law equation. Jackson [23] theorized the physical meaning of d as the centre height of the moment of drag force acting on a rough surface. Based on this theory, d is calculated from experimental measurement of pressure drag. Hence, the "one-parameter fitting" method was introduced and adopted by Leonardi et al. [24] and Cheng et al. [7]. In this study, the Jackson's [23] definition of d is interpreted as a similar parameter with different notation which is H_c as mentioned earlier. One-parameter fitting is also adopted by authors for comparison with other methods.

Lastly, in the fifth approach, d is determined on the basis of Jackson's theory using the highly precise data obtained by direct numerical simulation (DNS), where z_o and von Karman's constant κ are simultaneously estimated based on log-law profile (e.g., Leonardi and Castro [25]). According to Leonardi and Castro [25], the von Karman's constant κ actually varies between 0.41 and 0.36 as λ_p increases.

The availability of these different approaches has called for analytical comparison to determine which one would suit best for a particular case of study. Several simplified prediction methods of the parameters z_o and d have been published based on theoretical and empirical approaches. Petersen [26] performed statistical comparison among seven different methods to estimate z_o through the measurement of velocity profile based on wind tunnel experiment. The arrays comprised of cubes and were mixed of two cube sizes in a staggered layout for λ_p = 0.69% and irregular layout. Although the method of Lettau [27] was favoured against other methods, it was deduced that its applicability is restricted to moderately inhomogeneous roughness arrays.

Macdonald et al. [28] and other researchers (Lettau [27], Counihan [29], Raupach [30], [31], Theurer [32], Kastner-Klein and Rotach [33]) introduced simple mathematical expressions to determined z_o and d based on the frontal area density, λ_f and/or plan area density, λ_p. Basically, λ_f and λ_p are defined as the ratios of building frontal area to ground surface area and of building plan area to ground surface area, respectively. Bottema [34] showed that z_o and d of cubical square and staggered arrays depend not only on λ_f but the layout pattern and streamwise building length are also influential parameters. Duijm [35] developed a mathematical equation to predict z_o and d for non-uniform obstacles with frontal area densities λ_f = 0–0.5% by extending the method proposed by Bottema ([36], [37]). On the other hand, Kondo and Yamazawa [38] developed a simple method to determine z_o for two cities in Japan without wind velocity measurement. They reported that z_o is proportional to the average size of the roughness elements. De Bruin and Moore [39] used analytical method based on mass conservation law on

the logarithmic wind profile to derive z_o and d for vegetation. They considered the existence of a transition layer above the vegetation therefore the measurement level was only needed to be within the inertial sub-layer. However, their approach could only be used for specified λ_f in sparse condition.

In addition, Grimmond and Oke [40] reviewed a large number of related studies and compared their results with the datasets for 11 spots in seven North American sites. They recommended the methods presented by Macdonald et al. [28] and Bottema [34] because the former has the advantage of providing reasonable estimates across a wide range of surface densities whilst the latter has an added applicability to different spatial arrays.

In light of prior work, the aim of this study is to determine the centre height of moment of drag force experimentally. The parameter d is determined by applying one-parameter fitting and two-parameter fitting and values from both methods are compared with each other and relevant available data from past researches. In Section 2, details of experimental set-up are described in terms of roughness arrays used and instrumentation for data measurement. In Section 3, experimental results are presented along with other data for comparison. The results are discussed based on what methods provide better estimates and justifications of data behaviour. Finally, in Section 4, significant results are summarized and conclusions based on this study are drawn.

2. Experimental Set-up

2.1. Wind tunnel device

The experiments were carried out in a low-speed single-return wind tunnel with a working section of 1 m high × 8 m long, which was located at the laboratory of the Interdisciplinary Graduate School of Engineering Sciences, Kyushu University, Japan. A schematic diagram of the wind tunnel is shown in Fig. 1. The surrounding of the floating element area was covered with a roughness array of lengths 3 m in the windward direction and 0.35 m in the leeward direction. In the windward direction, the length of 3 m is equal to 120 times the height of block, which is sufficient for the development of equilibrium layer (Hagishima et al. [14]). In addition, Cheng and Castro [5] investigated the influence of fetch on the development of equilibrium layer and deduced that the fetch needs to be around 300 times roughness length in a condition of 5% difference in velocity. Regardless, this study adopted the same value used in Hagishima et al. [14].

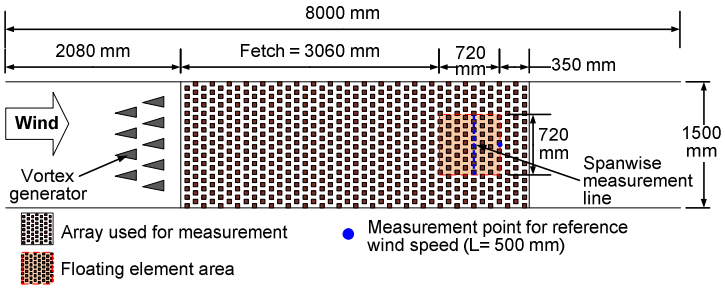

Fig. 1. Schematic of Wind Tunnel Experimental Set-up.

2.2. Configuration of roughness array

The schematic plan view of block arrays with layouts of staggered (hereafter ST1), square (hereafter SQ1), and diamond (hereafter D1) is shown in Fig. 2. All blocks are 25 mm cubes with sharp edges from which we assume H = 25 mm as a standard length scale.

In this study, the measurement was carried out for three different packing densities of λ_p (7.7%, 17.4%, and 30.9%) for the arrays of ST1, SQ1, and D1. Table 1 shows the summarized details of the measured arrays.

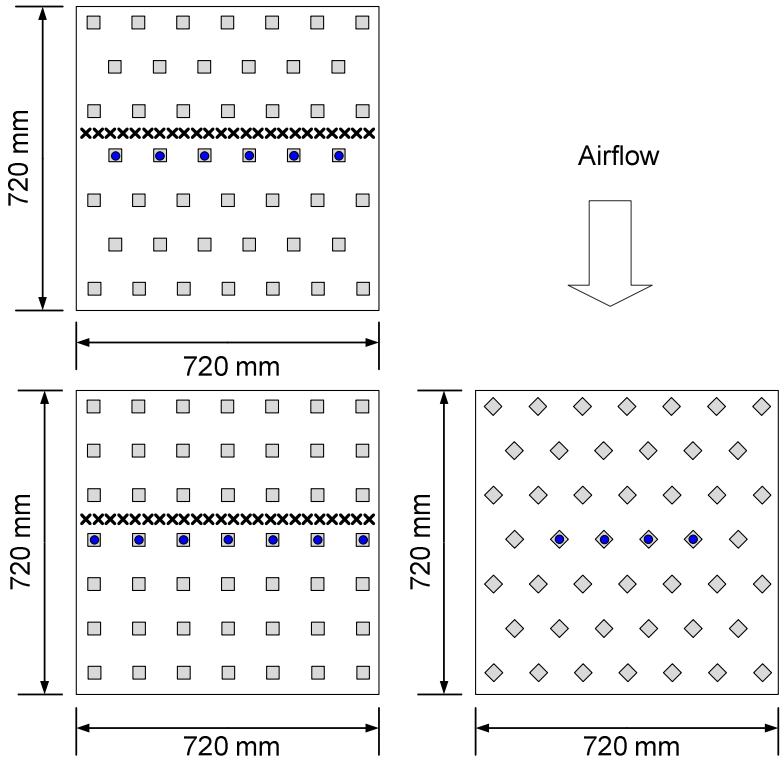

Fig. 2. Schematic Plan View of Roughness Elements with λ_p = 7.7%.
(Black circles indicate the measurement cubes of pressure drag. Crosses refer to the measurement points of spanwise velocity at heights of 3*H*, 8*H*, and 20*H*.)

Table 1. Roughness Array Condition.

Array	Layout	Remarks
ST1	**Staggered**	**Cubical arrays ($L \times L \times L$), $H = L$**
SQ1	**Square**	
D1	**Diamond**	**Cubical 45° rotated array with staggered array.**

H is the height of cubes and L is the width of all cubes (L = 25 mm).

2.3. Measurement items and instrument

To perform pressure drag measurements, a wooden cube was swapped with the one that was fitted with 25 pressure tappings on its vertical face as shown in Figs. 3 and 4. These tappings were then connected to a 16-port pressure scanner (Scanivalve, DSA 3217) by tubes. The digitized signal from the scanner was transmitted to a computer that was installed with DSA 3000 software for data analysis. The wind pressure coefficient was obtained from the differential of pressures on the windward and leeward walls. These two values were obtained from the two different settings installed on the tapping block.

A Pitot-static tube connected to the pressure scanner aforementioned was used to record reference flow speed at 20*H*; the static pressure was used as the reference pressure for the wall pressure measurement. The pressure measurement was performed after a warm-up period of about one hour and calibration was done at zero pressure. The sampling frequency and sampling time at each measurement point were 200 Hz and 50 s respectively. The authors did the pressure drag measurement three times for each tapping and used the average values in the following analysis.

The pressure drag acting on individual cubes was approximated as an ensemble average of cubes located in the spanwise direction as shown in Fig. 2 in order to obtain the accurate representative value of the array. All measurements described here were carried out in a freestream velocity of about 8 ms^{-1}. The wind pressure coefficient on a wall of a cube is defined as:

$$C_p = \frac{P_f - P_b}{\frac{1}{2}\rho U_{ref}^2} \tag{4}$$

where P_f and P_b are the pressure on the front and back faces respectively; U_{ref} is the reference mean speed at a height of z; and ρ is the density of air.

To clarify the spanwise large scale fluctuation of mean velocity in the wind tunnel, the authors performed another experiment of mean wind speed at 3*H*, 8*H*, and 20*H* using a split-film anemometry in the previous study (Zaki et al. [41]). The results obtained show consistency between the variations in the pressure drag and the velocity. Furthermore, similarly to the results of Reynolds et al. [42], the amplitude of the fluctuation in the pressure drag matches with that in the velocity (Zaki et al. [41]). Needless to say, both experiments were conducted on a fully rough surface with roughness Reynolds number Re* of greater than 5 which is preferable for insignificant viscous effects (Snyder and Castro [43]).

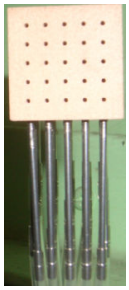

Fig. 3. The Pressure Tap Cube Having 25 Pressure Tapping Points.

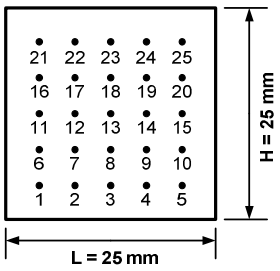

Fig. 4. Pressure Tapping Distribution on the Cube.

2.4. Distribution of pressure drag on walls

The pressure drag measurement (Cheng et al. [7] and Zaki et al. [44]) can be used to derive the centre of height of the moment of drag force H_c using the following expressions:

$$H_c = \frac{\overline{M}}{\overline{\Delta P}} \tag{5}$$

$$\overline{M} = \frac{\sum_{i=1}^{n}\left(P_{fi} - P_{bi}\right)z_i}{n} \tag{6}$$

$$\overline{\Delta P} = \frac{\sum_{i=1}^{n}\left(P_{fi} - P_{bi}\right)}{n} \tag{7}$$

where $\overline{M}$ is the average of the moment; $\overline{\Delta P}$ is the average of the pressure difference; P_{fi} and P_{bi} are the pressures on the front and back faces of a pressure tapping i, respectively; z_i is the height of pressure tapping i; and n is the total number of pressure tapings on the cube.

In our preceding study (Hagishima et al. [14]), z_o and d were estimated based on the log-law fitting (hereafter, we refer to this method as the "two-parameter fitting"). In the present study, based on the assumption that H_c is equal to d (hereafter the one-parameter fitting), z_o is recalculated using the nonlinear least-squares method. z_o is optimized by satisfying the minimum sum of error of mean wind speed E which is determined as follows:

$$E = \frac{1}{\left(t-b+1\right)}\sum_{i=b}^{t}\left(\frac{U_i - \frac{u_*}{\kappa}\ln\left(\frac{z_i - H_c}{z_o}\right)}{U_i}\right)^2 \tag{8}$$

where U_i is the measured wind speed at height z_i; z_b and z_t are the respective lowest and highest levels for the mean wind measurement from the selected region between 1.5H to 7H, which are used for the determination of parameters. This procedure is similar to that used by Cheng et al. [7] and Hagishima et al. [14].

3. Result and Discussion

3.1. Streamwise velocity profiles

Figure 5 shows the comparison of wind profiles between measured and estimated results for staggered, square, and diamond arrays. It is shown in the plots that the estimated log-law lines fit the experimental data through the roughness sub-layer and inertial sub-layer. For the staggered array, the value of one-parameter fitting that is H_c as the displacement height shows better fitting whereas for square and diamond arrays, the value of two-parameter fitting is more accurate. Staggered arrays are somehow more aerodynamically rough than square or diamond arrays so the more suitable approximation of its velocity profile would be the one-parameter fitting that incorporates the measurement of pressure drag which is an

important parameter due to its more drag-inducing condition according to Cheng and Castro [5].

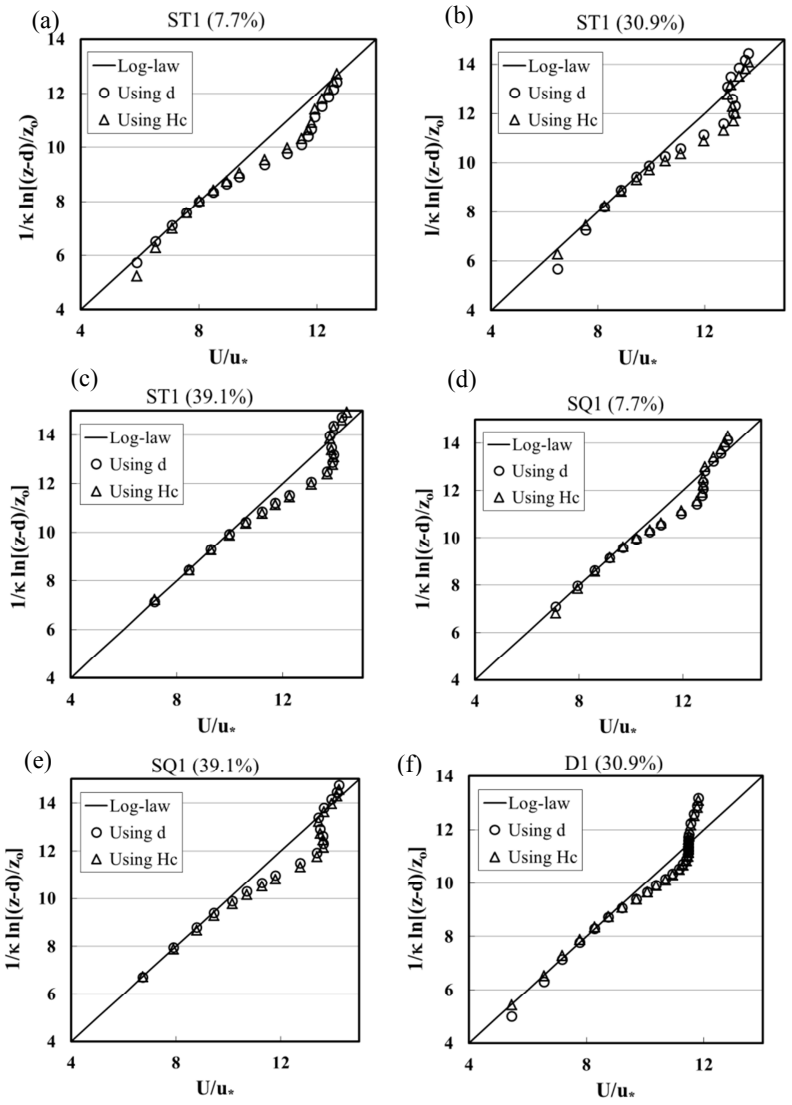

Fig. 5. Fitted Log-law Profiles for Staggered, Square, and Diamond Array.

3.2. Centre height of the moment of drag force and roughness length

The estimated H_c and z_o normalized by block height H are shown in Fig. 6. The displacement height presented by Hagishima et al. [14] is plotted as a reference, while the previous work from Macdonald et al. [28], Kanda et al. [21], Cheng et al. [7], and Leonardi and Castro [25] are also shown for comparison.

The estimated H_c/H values for staggered and square arrays are significantly lower than d/H, except for the lowest packing density. This is particularly due to the higher pressure difference at low roughness density than at high roughness density which is understandably caused by less interference effects; subsequently, this leads to high H_c value. This behaviour is consistent with the results of cubical staggered array using large-eddy simulation (LES) reported by Leonardi and Castro [25]. A similar trend is also found by Kanda et al. [18] for square array and Cheng et al. [7] for aligned and staggered arrays with various packing densities. However, the trend of the curve of λ_p–H_c/H is slightly different from the well-known prediction by Macdonald et al. [28], which exhibits a convex increase of d.

The inconsistencies observed between the theoretical prediction made by Macdonald et al. [28], present data, and previously available data showed d and H_c somehow are not similar in their physical meaning. Although at high packing density, i.e., 40% the values of H_c/H from the present study and d/H from the prediction by Macdonald et al. [28] for square array showed slight agreement, but the rest of the results do not follow this trend.

This disagreement between data has been explained in previous literatures. Kanda et al. [18] and Leonardi et al. [24] reported that the centre at which the form drag acts H_c does not coincide with the displacement height obtained by the two-parameter fitting method due to the existence of the recirculation regime within the canopy layer. In addition, Leonardi and Castro [25] supported Jackson's theory and pointed out that the seeming discrepancy between H_c and d is caused by the fact that the von Karman's coefficient is not universal, but varies with λ_p due to the flow characteristics around blocks.

The z_o/H values of the three arrays based on one-parameter fitting are slightly larger than the data derived by two-parameter fitting (Hagishima et al. [14]) when $\lambda_p \geq 31\%$. This observation is attributed to the lower corresponding value of displacement height at high packing density which eventually contributes to the increase of roughness length. The results are consistent with the results of the staggered and aligned arrays for $\lambda_p = 25\%$ presented by Cheng et al. [7]. The discrepancy of z_o/H for the staggered and diamond arrays between one-parameter and two-parameter fittings is relatively high for λ_p = 7.7%. In contrast, the discrepancy of the two methods of staggered array for λ_p = 6.25% reported by Cheng et al. [7] is extremely low. This result might be due to the insufficient measurement points of wind speed to obtain a spatially averaged profile under the condition of sparse density. Therefore, for next experimental studies, the number of measurement points should be increased for more accurate spatial averaging of wind speed.

According to the report by Leonardi and Castro [25], not only the directly measured H_c, but also modification of von Karman's coefficient resulted in a good log-law fitting. Considering the present result, it is necessary to improve the measurement method of mean wind distribution for further experimental determination of z_o of various types of arrays, to obtain a more precise spatially averaged profile.

In Fig. 6. ST1 (Ha) and SQ1 (Ha) refer to the value for staggered and square cubical arrays (Hagishima et al. [14]). ST1 (Cheng) and AL1 (Cheng) refer to the estimation by Cheng et al. [7] for staggered and aligned cubical array. ST1 (Ma) refers to the previous work by Macdonald et al. [28] with prediction by semi-

empirical method. SQ1 (Kanda) refers to the estimation by Kanda et al. [18] for cubical square array based on logarithmic fitting using the results of LES. ST1 (L&C) denotes the LES method adopted by Leonardi and Castro [25].

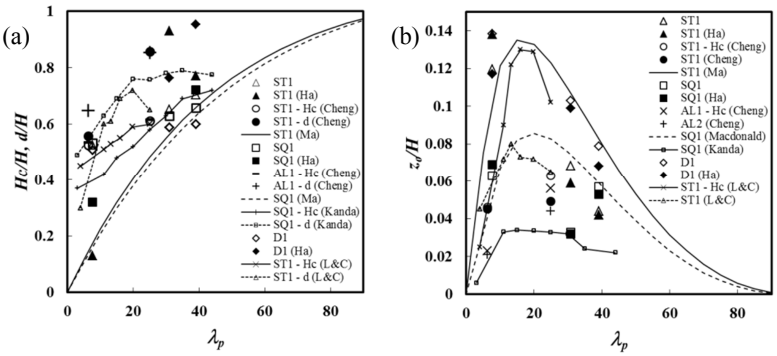

Fig. 6. Aerodynamic Parameters Estimated from the Height of Centre of Drag, H_c, for Regular Arrays with Different λ_p.

4. Conclusions

A series of wind tunnel experiments was performed using rectangular blocks arrays arranged in staggered, square, and diamond layouts with various roughness packing densities to measure the spatial distribution of the wind pressure coefficient (C_p) acting on the walls of blocks.

The authors derived the height of a centroid of pressure drag H_c for each array and recalculated z_o using one-parameter fitting by assuming that H_c is identical to displacement height d. The slope of H_c/H versus λ_p plotted for the three arrays slightly increases when λ_p is less than 39.1%. Notably, this trend is different from the convex-increasing trend reported by Macdonald et al. [28]. On the other hand, the estimated H_c/H values for the staggered and square arrays are significantly lower than d/H, except for the lowest packing density; and such trend is consistent with that observed in previous studies (Leonardi and Castro [25] and Cheng et al. [7]). This explains the pressure difference on the walls of blocks is higher in sparse arrays due to less interference effect as opposed to dense arrays of which H_c values were measured lower.

In addition, the authors compared the estimated H_c and z_o with our previous data (Hagishima et al. [14]), which is based on the simultaneous log-law fitting of z_0 and d or two-parameter fitting. The fact that the z_o/H values of the three arrays based on one-parameter fitting are slightly larger than the data derived by two-parameter fitting for $\lambda_p \geq 31\%$ is most likely caused by lower value of displacement height with one-parameter fitting at high packing density which eventually contributes to the increase of roughness length. Moreover, this could also explain the linear relationship between packing density and roughness length.

In this study, both fitting methods yield a deviating yet comparable set of data. In terms of understanding the physical meaning of d, at a range of low packing density, H_c could be computed as d. Still, the parameterization of z_o seems to yield reasonable results mainly due to the direct measurement of u^* and H_c of which its physical meaning is defined unlike d which is a fitting parameter in the

two-parameter fitting method. Nevertheless, the present results suggest that both accurate measurements of spatially averaged wind profile and direct measurement of H_c are useful for further experimental determination of the roughness length and displacement height of an array.

Acknowledgements

This research was financially supported by Grant-in Aid for Scientific Research (22360238) from the Ministry of Education, Science and Culture of Japan and the Malaysian Ministry of Higher Education (MOHE) under the Fundamental Research Grant Scheme (FRGS) project.

References

1. Claus, J.; Krogstad, P.-A.; and Castro, I.P. (2012). Some measurements of surface drag in urban-type boundary layers at various wind angles. *Boundary-Layer Meteorology*, 145(3), 407-422.
2. Kanda, M.; Inagaki, A.; Miyamoto, T.; Gryschka, M.; and Raasch, S. (2013). A new aerodynamic parameterization for real urban surfaces. *Boundary-Layer Meteorology*, 148(2), 357-377.
3. Cook, N.J, (1977/78). Determination of the model scale factor in wind tunnel simulations of the atmospheric boundary layer. *Journal of Wind Engineering and Industrial Engineering*, 2(4), 311-321.
4. Iyengar, A.K.S.; and Farell, C. (2001). Experimental issues in atmospheric boundary layer simulations: roughness length and integral length scale determination. *Journal of Wind Engineering and Industrial Aerodynamics*, 89(11-12), 1059-1080.
5. Cheng, H.; and Castro, I.P. (2002). Near wall flow over urban-like roughness. *Boundary-Layer Meteorology*, 104(2), 229-259.
6. Salizzoni, P.; Soulhac, L.; Mejean, P.; and Perkins, R.J, (2008). Influence of a two-scale surface roughness on a neutral turbulent boundary layer. *Boundary-Layer Meteorology*, 127(1), 97-110.
7. Cheng, H.; Hayden, P.; Robins, A.G.; and Castro, I.P. (2007). Flow over cube arrays of different packing densities. *Journal of Wind Engineering and Industrial Aerodynamics*, 95(8), 715-740.
8. Feddersen, B. (2004). *Wind tunnel modelling of turbulence and dispersion above tall and highly dense urban roughness*. PhD thesis, Swiss Federal Institute of Technology, Zurich, p. 211.
9. Raupach, M.R.; Hughes, D.E.; and Cleugh, H.A. (2006). Momentum absorption in rough-wall boundary layers with sparse roughness elements in random and clustered distributions. *Boundary-Layer Meteorology*, 120(2), 201-218.
10. Padhra, A. (2009). *Estimating the sensitivity of urban surface drag to building morphology*. Ph.D. Thesis University of Reading, p. 143.
11. Von Karman (1921). Über laminare und turbulente Reibung. *ZAMM: Zeitschrift für Angewandte Mathematik und Mechanik* (*Journal of Applied Mathematics and Mechanics*), 1(4), 233-253. English Translation in NACA TM 1092.

12. Maruyama, T. (1993). Optimization of roughness parameters for staggered arrayed cubic blocks using experimental data. *Journal of Wind Engineering and Industrial Aerodynamics*, 46-47, 165-171.
13. Mochizuki, S.; Kameda, T.; and Osaka, H. (2006). Self-preservation of a turbulent boundary layer over d-type roughness. *Journal of Fluid Science Technology*, 1(1), 24-35.
14. Hagishima, A.; Tanimoto, J.; Nagayama, K.; and Meno, S. (2009). Aerodynamic parameters of regular arrays of rectangular blocks with various geometries. *Boundary-Layer Meteorology*, 132(2), 315-337.
15. Zaki, S.A.; Hagishima, A.; Tanimoto, J.; and Ikegaya, N. (2011). Aerodynamic Parameters of Urban Building Arrays with Random Geometries. *Boundary-Layer Meteorology*, 138(1), 99-120.
16. Antonia, R.A.; and Luxton, R.E. (1971). The response of a turbulent boundary layer to a step change in surface roughness Part 1. Smooth to rough. *Journal of Fluid Mechanics*, 48(4), 721-761.
17. Theurer, W.; Baechlin, W.; and Plate, E.J. (1992). Model study of the development of boundary layers above urban areas. *Journal of Wind Engineering and Industrial Aerodynamics*, 41(1-3), 437-448.
18. Kanda, M.; Moriwaki, R.; and Kasamatsu, F. (2004). Large eddy simulation of turbulent organized structure within and above explicitly resolved cube arrays. *Boundary-Layer Meteorology*, 112(2), 343–368.
19. Coceal, O.; Thomas T.G.; Castro I.P.; and Belcher S.E. (2006). Mean flow and turbulence statistics over groups of urban-like cubical obstacles. *Boundary-Layer Meteorology*, 121(3), 491-519.
20. Jiang, D.; Jiang, W.; Liu, H.; and Sun, J. (2008). Systematic influence of different building spacing, height and layout on mean wind and turbulent characteristics within and over urban building arrays. *Wind and Structures*, 11(4), 275-289.
21. Kanda, M.; and Moriizumi, T. (2009). "Momentum and heat transfer over urban-likes surfaces. *Boundary-Layer Meteorology*. 131(3), 385-401.
22. Tomas, S.; Eiff, O.; and Manson, V. (2011). Experimental investigation of turbulent momentum transfer in a neutral boundary layer over a rough surface. *Boundary-Layer Meteorology*, 138(3), 385-411.
23. Jackson, P.S. (1981). On the displacement height in the logarithmic velocity profile. *Journal of Fluid Mechanics*, 111, 15-25.
24. Leonardi, S.; Orlandi, P.; Smalley, R.J.; Djenidi, L.; and Antonia, R.A. (2003). Direct numerical simulations of turbulent channel flow with transverse square bars on one wall. *Journal of Fluid Mechanics*, 491, 229-238.
25. Leonardi, S.; Castro, I.P. (2010). Channel flow over large cube roughness: a direct numerical simulation study. *Journal of Fluid Mechanics*, 651, 519-539.
26. Petersen, R.L. (1997). A wind tunnel evaluation of methods for estimating surface roughness length at industrial facilities. *Atmospheric Environment*, 31(1), 45-57.
27. Lettau, H. (1969). Note on aerodynamic roughness-parameter estimation on the basis of roughness-element description. *Journal of Applied Meteorology*, 8(5), 828-832.
28. MacDonald, R.W.; Griffiths, R.F.; and Hall, D.J. (1998). An improved method for estimation of surface roughness of obstacle arrays. *Atmospheric Environment*, 32(11), 1857-1864.

29. Counihan, J. (1971). Wind tunnel determination of the roughness length as a function of the fetch and the roughness density of three-dimensional roughness elements. *Atmospheric Environment*, 5(8), 637-642.
30. Raupach, M.R. (1992). Drag and drag partition on rough surfaces. *Boundary-Layer Meteorology*, 60(4), 375-395.
31. Raupach, M.R. (1994). Simplified expressions for vegetation roughness length and zero-plane displacement as functions of canopy height and area index. *Boundary-Layer Meteorology*, 71(1-2), 211-216.
32. Theurer, W. (1993). *Dispersion of ground level emissions in complex built-up areas*. PhD thesis, University of Karlsruhe, Germany.
33. Kastner-Klein, P.; and Rotach, M.W. (2004). Mean flow and turbulence characteristics in an urban roughness soublayer. *Boundary-Layer Meteorology*, 111(1), 55-84.
34. Bottema, M. (1997). Urban roughness modelling in relation to pollutant dispersion. *Atmospheric Environment*, 31(18), 3059-3075.
35. Duijm, N.J. (1999). Estimates of roughness parameters for arrays of obstacles. *Boundary-Layer Meteorology*, 91(1), 1-22.
36. Bottema, M. (1995). Aerodynamic roughness parameters for homogeneous building groups, part 1: theory, DOCUMENT SUB-MESO#18 and part 2: results, DOCUMENT SUB-MESO#23. *Report, Ecole Centrale de Nantes, France*, 80.
37. Bottema, M. (1996). Roughness parameters over regular rough surfaces: experimental requirements and model validation. *Journal of Wind Engineering and Industrial Aerodynamics*, 64(2-3), 249-265.
38. Kondo, J.; and Yamazawa, H. (1986). Aerodynamic roughness over an inhomogeneous ground surface. *Boundary-Layer Meteorology*, 35(4), 331-348.
39. De Bruin, H.A.R.; and Moore, C.J. (1985). Zero-plane displacement and roughness length for tall vegetation, derived from a simple mass conservation hypothesis. *Boundary-Layer Meteorology*, 31(1), 39-49.
40. Grimmond, C.S.B.; and Oke, T.R. (1999). Aerodynamic properties of urban areas derived from analysis of surface form. *Journal of Applied Meteorology*, 38(9), 1262-1292.
41. Zaki, S.A.; Hagishima, A.; and Tanimoto, J. (2012). Experimental study of wind-induced ventilation in urban building of cube arrays with various layouts. *Journal of Wind Engineering and Industrial Aerodynamics*, 103, 31-40.
42. Reynolds, R.T.; Hayden, P.; and Castro, I.P. (2007). Spanwise variations in nominally two-dimensional rough-wall boundary layers. *Experiments in Fluids*, 42(2), 311-320.
43. Synder, W.H.; and Castro, I.P. (2002). The critical Reynolds number for rough-wall boundary layer. *Journal of Wind Engineering and Industrial Aerodynamics*, 90(1), 41-54.
44. Zaki, S.A.; Hagishima, A.; and Tanimoto, J. (2011). Spatial distribution of pressure drag acting on rectangular block arrays with various layouts. *Proceedings of Building Simulation 2011: 12th Conference of International Building Performance Simulation Association*, Sydney, 14-16 November, 1686-1693.